The International Journal of Advanced Manufacturing Technology (2019) 103:2941–2951
https://doi.org/10.1007/s00170-019-03677-3

ORIGINAL ARTICLE

Deformation characteristics of self-infeed rolling process for thread shaft

Shuowen Zhang[1] · Shuqin Fan[1,2] · Qi Wang[1] · Shengdun Zhao[1] · Qian Zhu[1]

Received: 3 September 2018 / Accepted: 29 March 2019 / Published online: 30 April 2019

Abstract

In this paper, the self-infeed rolling process of thread shaft with medium carbon steel AISI 1045 is investigated. Firstly, the principle of the self-infeed rolling process is introduced and then the deformation mechanism is analyzed by finite element method. The numerical results show that deformation mainly occurs on the surface layer of blank, and the deformation degree is different in the tooth profile. The metal flows along both the axial direction and the radial direction. Next, the experimental studies of self-infeed rolling process are carried out. The numerical results are shown in good accordance with the experimental results. The grain at the top of tooth profile is refined, and the microstructures in the surface of tooth profile as well as bottom of tooth root are fibrous tissue which is dense and streamlined obviously. The hardness of the formed thread shaft is improved than that of the blank.

Keywords Thread shaft · Self-infeed rolling process · Deformation mechanism · Finite element analysis · Experiments

1 Introduction

Thread shafts are widely applied to transmit torque and motion in the mechanical industry. The forming operations and machining operations are all carried out in the process of threads manufacturing. Forming process of threads is similar with forming spline shafts [1, 2] and gears [3, 4]. Formed thread shaft exhibits economic and technological advantages comparing with machining operations. These advantages include high strength, high reliability, and material saving [5].

The traditional forming process of thread shaft can be classified into two types: forming process with flat dies and that with round dies. Figures 1 and 2 show the traditional forming process applied in thread shaft. In flat dies forming process, the blank is placed between the up screw die and down screw die. When the rolling process begins, the up screw die moving and the blank is formed thread shaft. In traditional forming process with round dies, the blank is rotated around its own axis, the round dies gradually infeed along the radical direction and rotate around their own axes.

In the early days, the method of trial machining was widely applied in the rolling process for manufacturing threads which was time consuming and severely relying on experience [6]. To improve the quality of thread and save the time and material, the finite element method was applied in thread manufacturing.

The forming process of grooves was firstly modeled by Martin [7]. By using the method of mesh discretization, the material displacement and the residual stress were predicted. Domblesky and Feng numerically studied the effect of geometrical, material, and frictional variations in the radial-infeed rolling process through two dimensions and the experimental verification with numerically calculated hardness values were matched [8]. And then, Domblesky and Feng tried to work on the three-dimensional modeling of radial-infeed rolling process, but due to the limitation of processing capabilities, the results of the numerical model were undesirable [9]. In this stage, the two-dimensional models were established but the number of mesh was small which led to the low accuracy of simulation.

Currently, most of the studies focus on the radial-infeed rolling process. The deformation characteristic by radial rolling process with flat die and round die has been studied. In these studies, the qualitative analysis of deformation

✉ Shuqin Fan
sunnyfan@xjtu.edu.cn

[1] School of Mechanical Engineering, Xi'an Jiaotong University, No.28 Xian Ning West Road, Xi'an, People's Republic of China

[2] State Key Laboratory of Materials Processing and Die & Mould Technology, Huazhong University of Science and Technology, No.1037 Luoyu Road, Wuhan, People's Republic of China

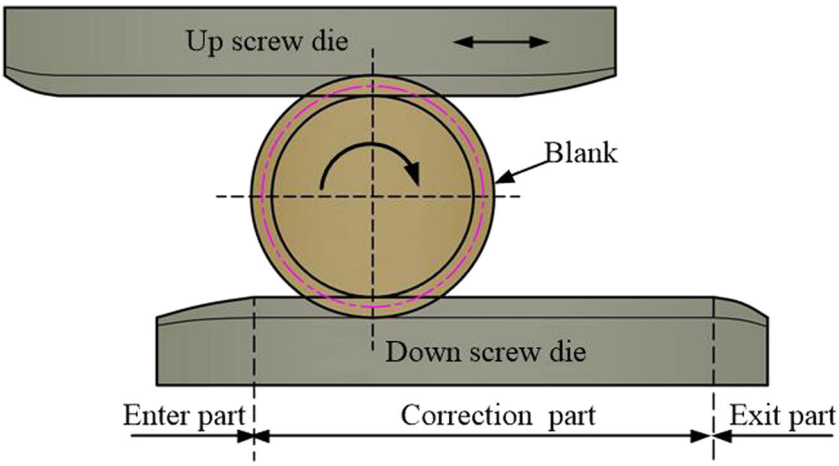

Fig. 1 The schematic diagrams of traditional rolling process of thread shaft with flat dies

characteristics of thread was carried out. Peter et al. firstly modeled a three dimension of sleeper screw forming process in 2004 [10]. From then on, Chen et al. [11] and Lee et al. [12] published further studies focusing on the numerical modeling of external thread. Qi et al. studied the hollow threads in radial-infeed cold rolling process by theoretical and experimental methods [13, 14]. Yamanaka et al. studied the influence of residual stress on elastic plastic behavior of metallic glass bolts formed through cold rolling process [15]. Nitu et al. using simulation and experimental methods studied the radial force and hardness during the wedge rolling process [16]. Zhang et al. studied the motion characteristics between rolling dies and blank in radial-infeed rolling process, and established the motion function related to angular, transmission ratio and rotation angle [17].

Some methods were proposed by researchers to form the more complex threads. In their study, the quality of part is an important index. Pater et al. developed a new method of thread rolling with special grooves designed and the simulation was completed using finite volumes method and finite element method; furthermore, experimental tests were conducted in laboratory [10]. Zhang et al. proposed a novel thread and spline synchronous rolling process [18], and studied the deformation mechanism [19], motion characteristics, phase characteristic, and so on [20].

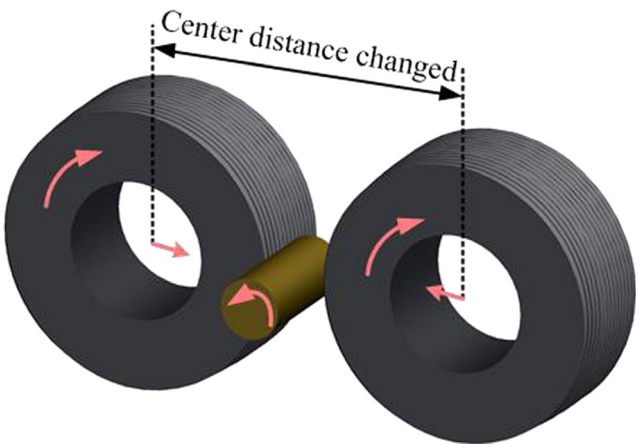

Fig. 2 The schematic diagrams of traditional rolling process of thread shaft with round dies

According to the above, as described, many studies focus on the radial-infeed rolling process. Although these traditional rolling processes can form thread shaft, many problems such as dies wear, huge forming load, and the limitation of length by dies remained to be solved. In order to solve these problems, the self-infeed rolling process of thread shaft is investigated in this paper. The self-infeed rolling process is an incremental forming process along the axial direction, which has the advantages: small forming load, sufficient of material flow, and unlimited length of forming thread shaft. The axial self-infeed rolling process as an important forming process for thread shaft rarely is studied. The strain, displacement, and material flow have significant effects on the performances of thread shaft.

In this paper, the finite element model and experiments are carried out. The deformation mechanism during self-infeed rolling process for thread shaft is quantitatively and qualitatively investigated. The behavior of material flow and equivalent strain are analyzed under specific conditions. In addition, the experiments of self-infeed rolling process are conducted and the microstructure of thread shaft and the shape of tooth profile are observed. The hardness of the formed thread shaft is also measured.

2 Principle of the self-infeed rolling process of thread shaft

As shown in Fig. 3, Fig. 3 a marked out the position of rolling die and blank, and the rolling die system mainly consists of rolling die-A, rolling die-B, and rolling die-C. Each rolling dies in self-infeed rolling die system includes three parts: the pre-rolling part, the correction part, and the exit part which are shown in Fig. 3b. The pre-rolling part with angle α_1 is

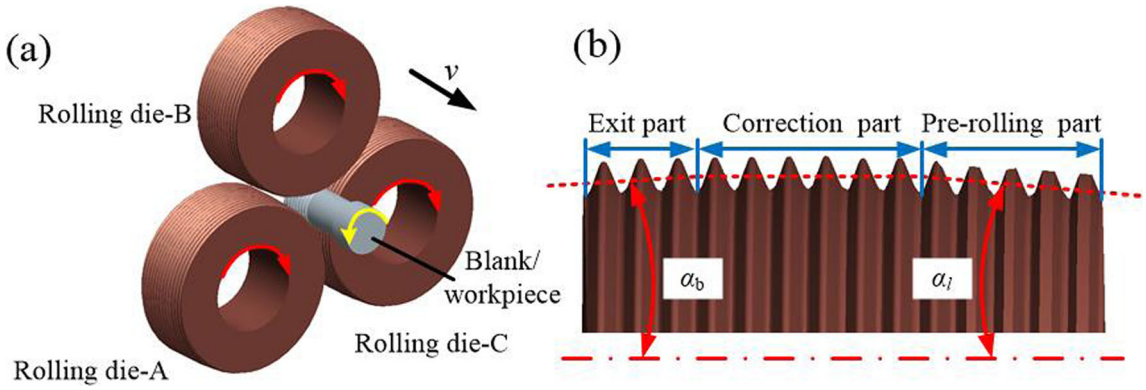

Fig. 3 The schematic diagrams of rolling dies. **a** rolling die system, **b** the local structure of rolling die

preforming for thread shaft. The function of correction part is adjustment for tooth profile and the exit part with angle α_b is convenient for the withdrawal of formed thread shaft.

The working process of self-infeed rolling process is shown in Fig. 4, and which includes the following steps: (1) Before the rolling process, the blank rotates with the speed n_b and the rolling dies remain stationary. (2) During the rolling process, when the rolling dies contact with the blank, the rolling dies begin to rotate with the speed n_d under the action of the meshing. The metal deformation occurs on the surface of the blank and the thread shaft is formed. (3) After the rolling process, the blank reversely rotates and the rolling dies retract along the axial direction until the formed thread part separates with rolling dies, the forming process ends.

3 Deformation process analysis by finite element method

3.1 Finite element models and process parameters

The thread shaft is investigated in this paper, and the material of blank is medium carbon steel AISI 1045. The blank diameter is 22.8 mm which is calculated according to the principle of constant volume during the plastic forming process. Three rolling dies are assembled into a rolling die system, and for each rolling die, the pre-rolling part angle α_l and exit part angle α_b are 3°, respectively. The pitch of rolling dies is 3 mm and the tooth angle is 60°. In the simulation, the Bauschinger effects and the elastic recovery of material are not taken into account and the rolling dies are regarded as rigid bodies. The rolling process is considered to be carried out at a constant temperature 20 °C and the effects of heat transfer among the blank, rolling dies, and environment are not considered. A Johnson–Cook model was applied in simulation. For the reason that the temperature did not increase remarkably during the cold rolling process, therefore, the Johnson–Cook constitutive model was expressed by Eq. 1.

$$\sigma = \left(A + B\varepsilon_p^n\right)\left(1 + C\ln\left(\frac{\dot{\varepsilon}}{\dot{\varepsilon}_0}\right)\right) \quad (1)$$

where σ is the yield stress and A, B, C, and n are material constants. The equivalent strain rate $\dot{\varepsilon}$ and the equivalent strain ε can be acquired from the simulation software, and $\dot{\varepsilon}_0$ is the reference strain rate. The parameters (A, B, C, and n) are obtained by tensile tests on INSTRON® universal mechanical testing machine and which show in Table 1.

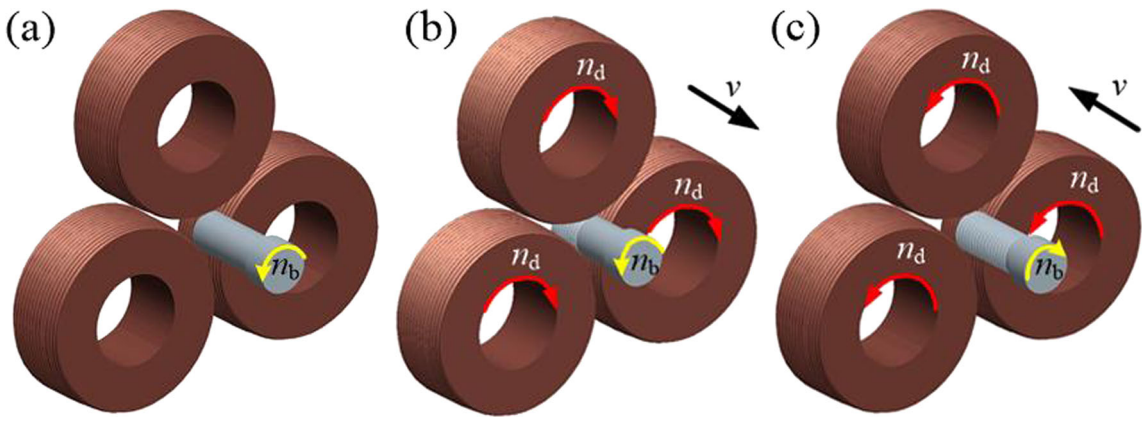

Fig. 4 The diagrams of self-infeed rolling process of thread shaft: **a** before rolling, **b** during rolling, and **c** after rolling

Table 1 Parameters in Johnson–Cook constitutive model

A	*B*	*C*	*n*
417.6	448.3	0.009	0.219

Based on the DEFORE-3D software, the simplified finite element models of self-infeed rolling process of thread shaft are present in Fig. 5a. Figure 5 b shows the grid discretization and the blank structure. On the surface of blank, the grid is refined to reduce its number and increase the accuracy of simulation, and the blank is quarter to save the computing resource. The mesh type is set as tetrahedral mesh, and the remeshing criterion is global remeshing, the relative interference depth is 0.7. And the minimum size of mesh is 0.02 mm. In this bulk forming process, Tresca yield criterion $\tau = mk$ was applied as the friction function, and the parameter m was set as 0.21 [21]. During the simulation, the time step is 0.05 s and the simulation step is 4000.

In practice, during the rolling process, the blank is rotating and the rolling dies only rotate around their own axes. But in the simulation, the blank is fixed through constrain surface. Therefore, the rolling dies need rotation and revolution to form the thread shaft. The speed of rolling dies rotate around their own axes is rotation speed and that of rolling dies rotate around the blank's axis is revolution speed which is equal to the rotating speed of the blank. The directions of rotation and revolution are identical. At the same time, the rolling die system infeeds along the axial direction; the speed is determined by the rotating speed of blank.

The revolution speed is referred the rolling speed in radial feed rolling process (when the pitch is 2 mm and the material is steel, the rolling speed is 20 r/min) [6]. In this simulation, the pitch is 3 mm and in order to reduce the forming torque, the rolling speed should be less than 20 r/min. Therefore, the revolution speed is set as 10 r/min. During the forming process, the blank contacts with the rolling dies, the linear velocities at pitch diameter of the formed thread shaft and the rolling die are same. The relationship can be expressed:

$$\omega_b d_b = \omega_r d_r \tag{2}$$

where ω_b is the angular velocity of the blank; d_b is the pitch diameter of the formed thread shaft. ω_r is the angular velocity of the rolling die; d_r is the pitch diameter of the rolling die. In this simulation, ω_b = 1.047 rad/s, d_b = 22.051 mm, d_r = 106.527 mm, therefore ω_r = 0.217 rad/s, the rotation speed v_r = 2.07 r/min.

So the kinematic parameters of finite element analysis are the rotation speed and the revolution speed of rolling die are 2.07 r/min and 10 r/min, respectively. The axial self-infeed velocity of rolling die system is 0.2923 mm/s, which is calculated according to the meshing theory.

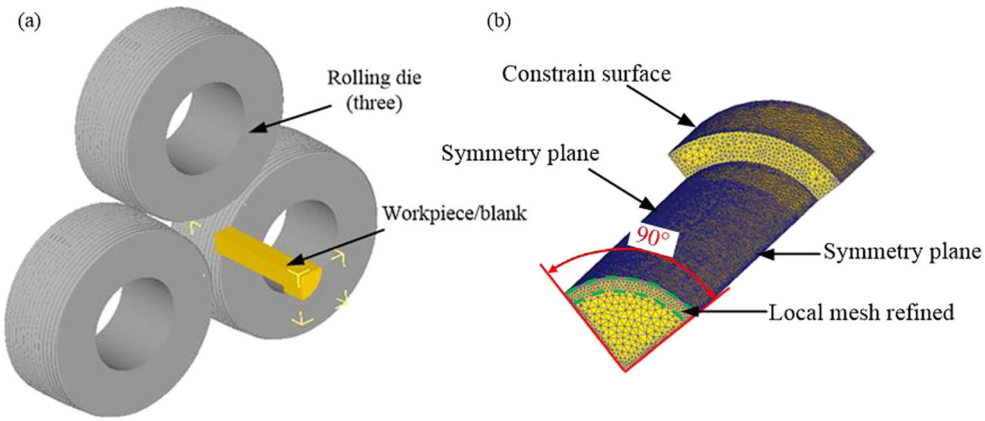

Fig. 5 Diagram of the finite element models: **a** finite element models and **b** the model of the blank and mesh

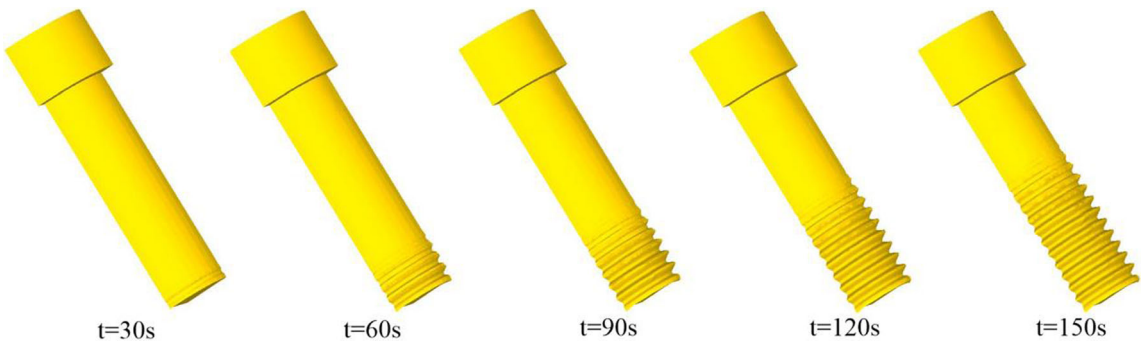

Fig. 6 The formation process of the thread shaft by self-infeed rolling process

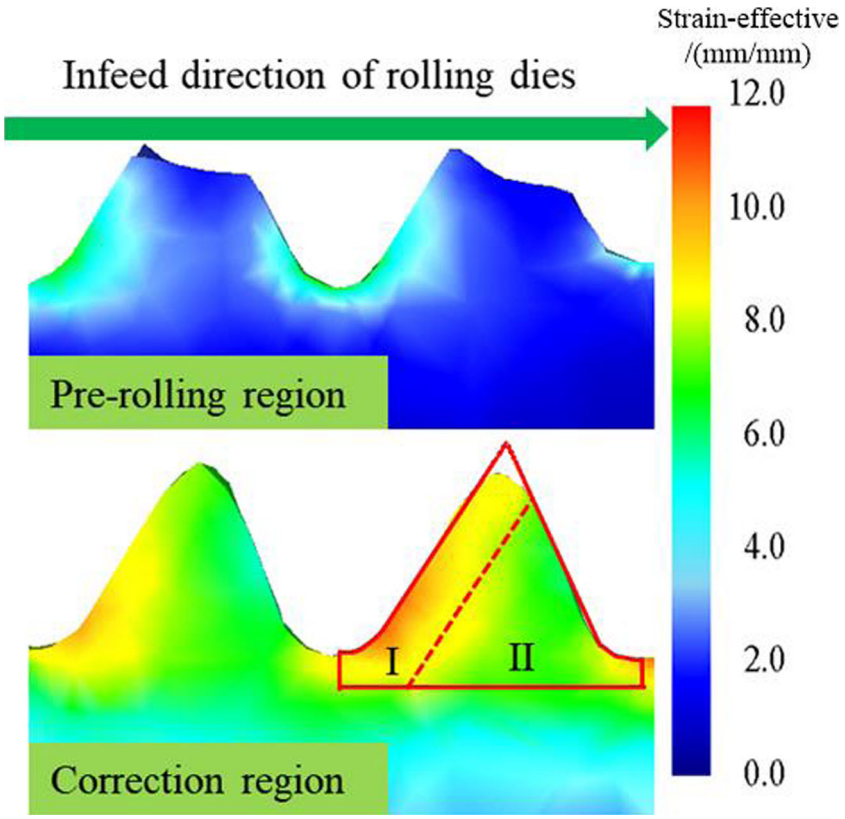

Fig. 7 The equivalent strain distribution of the formed thread shaft by self-infeed rolling process

Figure 6 shows the formation process of the thread shaft corresponding to different times through finite element analysis. Before 90 s, the pre-rolling part of rolling die contacts with the blank and the material on the surface of blank is formed indentation. After 90 s, the correction part of rolling die calibrates the formed indentation until the desired tooth profile is formed. In 150 s, the length of formed thread is equal to the width of the rolling die.

3.2 The equivalent strain distribution

From the distribution of the equivalent strain, the deformation degree in plastic forming process can be acquired. The equivalent strain exerts impact the work hardness, surface quality, and the fatigue strength of formed thread shaft. Figure 7 shows the equivalent strain distribution respectively in the pre-rolling region and the correction region. In the pre-rolling region, the equivalent strain mainly focus on the tooth space. The values of equivalent strain in the tooth profile and the center of workpiece are less. In the correction region, the maximum equivalent strain is located on the bottom of tooth space as well as at one side of tooth profile along the infeed direction of rolling dies. The equivalent strain of tooth profile is not uniformly distributed. In region I the equivalent strain is larger than that in region II, because the rolling dies in region I extrude the material more seriously for the action of pre-rolling angle and axial motion.

Figure 8 shows the equivalent strain values along the radius in the correction region. When the radius is less than 9.0 mm, the equivalent strain values are small (below 2.9), both along the tooth profile and tooth space directions. Along the tooth space direction, the equivalent strain values grow to 9.36 as the radius increases from 9.0 to 10.12 mm. Along the tooth profile direction, the equivalent strain values gradually increase to 7.94 when the radius is 11 mm. Then, the equivalent strain values become nearly

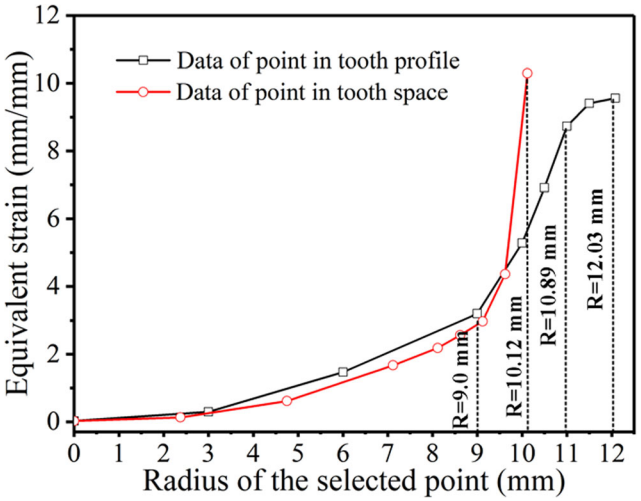

Fig. 8 The equivalent strain values with different radius of the formed thread shaft

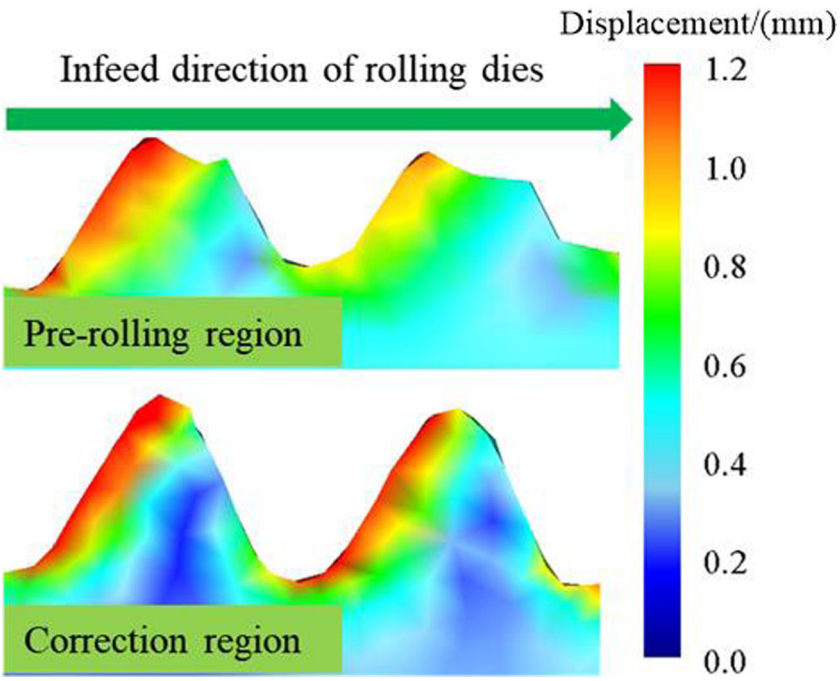

Fig. 9 The axial displacement distribution of formed thread shaft

constant as the radius increases from 11.4 to 12.03 mm. The value of the equivalent strain when the radius is 10.89 mm represents the boundary of deformation degree. The deformation degree almost remains unchanged and keeps at the maximum value once reached to or over the radius of 10.89 mm, indicating the primary thickness of affecting strain.

As a result, the characteristics of the equivalent strain distribution can be summarized as follows: the plastic deformation in the tooth space is larger than that in the tooth profile; the deformation degree of region I is larger than that of region II in the tooth profile; the deformation mainly occurs on the surface layer of thread shaft; and the deformation degree decreases along the inward radial direction.

3.3 The behavior of material flow

The material displacement of the formed thread shaft reflects the deformation accumulation degree of material during the self-infeed rolling process of thread shaft. Figure 9 shows the total displacement distribution of the thread shaft, and the total displacement distributions of the pre-rolling region and the correction region are presented. It is obvious that the displacement distributions of tooth profile are different and the displacement manly distributes on the surface of the formed thread shaft, which is corresponding to the equivalent strain distribution characteristic.

The values of axial material displacement and radial material displacement corresponding to different radiuses are respectively shown in Figs. 10 and 11. The different radius

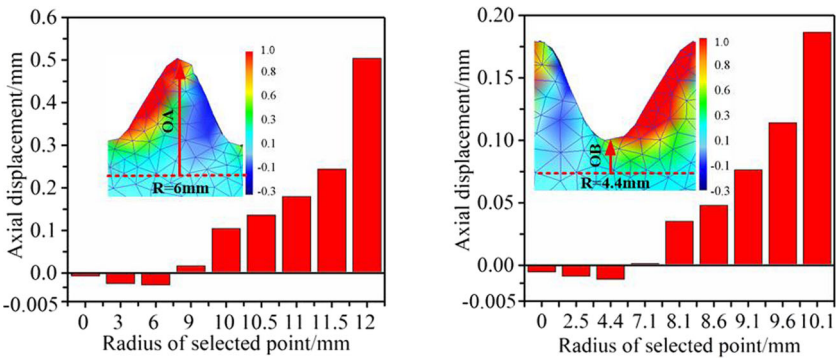

Fig. 10 The axial displacement of formed thread shaft. **a** The axial displacement distribution in tooth profile. **b** The axial displacement distribution in tooth space

(a) The axial displacement distribution in tooth profile

(b) The axial displacement distribution in tooth space

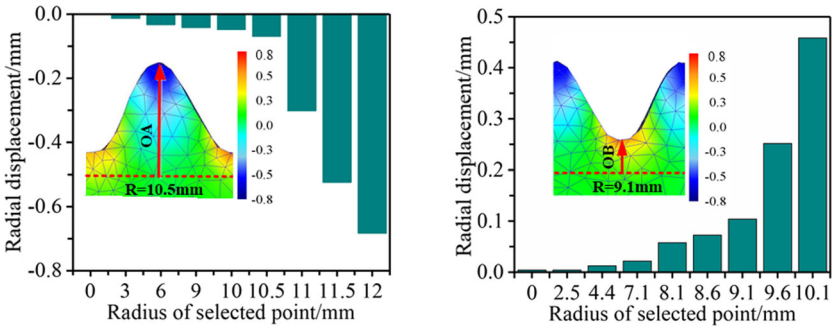

Fig. 11 The radial displacement of formed thread shaft. **a** The radial displacement distribution in tooth profile. **b** The radial displacement distribution in tooth space

(b) The radial displacement distribution in tooth profile

(b) The radial displacement distribution in tooth space

points along OA direction are selected in tooth profile and along OB direction in tooth space. Figure 10 a shows the axial displacement of different radius in tooth profile. When the radius is less than 6 mm, the axial displacement is negative but the values are very small. When the radius increases from 6 to 12 mm, the material displacement values increase to 0.51 mm. In Fig. 10b (in tooth space region), the axial displacement distribution is similar to that in tooth profile. The axial displacement is negative when the radius is less than 4.4 mm. The radius increase from 4.4 to 10.1 mm; the material displacement values increase to 0.18 mm.

The radial displacement values corresponding to different radius both in tooth profile and tooth space are shown in Fig. 12. Figure 12 (a) shows radial displacement values in tooth profile. When the radius is less than 10.5 mm, the absolute value of radial displacement is about 0.1 mm. As the radius increases from 10.5 to 12 mm, the absolute value of displacement values increase sharply from 0.31 to 0.69 mm. Figure 12 (b) shows the radial displacement values in tooth space. When the radius is less than 9.1 mm, the absolute value of radial displacement is below 0.1 mm. As the radius increases from 9.1 to 10.1 mm, the absolute value of displacement values sharply increase to 0.46 mm.

In summary, during the self-infeed rolling process of thread shaft, the material axial displacement and radial displacement mainly occur on the surface layer. In the core region, the material displacement is slightly. The axial displacement can lead to the elongation of formed thread shaft which has negative impact on formed precision. In the tooth profile, the axial displacement values and radial displacement values are larger than that in the tooth space.

During the rolling process, under the action of the surface force (rolling force), the strain and deformation are produced. In the bottom of the tooth space, the maximum deformation leads to the largest equivalent strain. So the material flows from the bottom of tooth space to the top of the tooth profile,

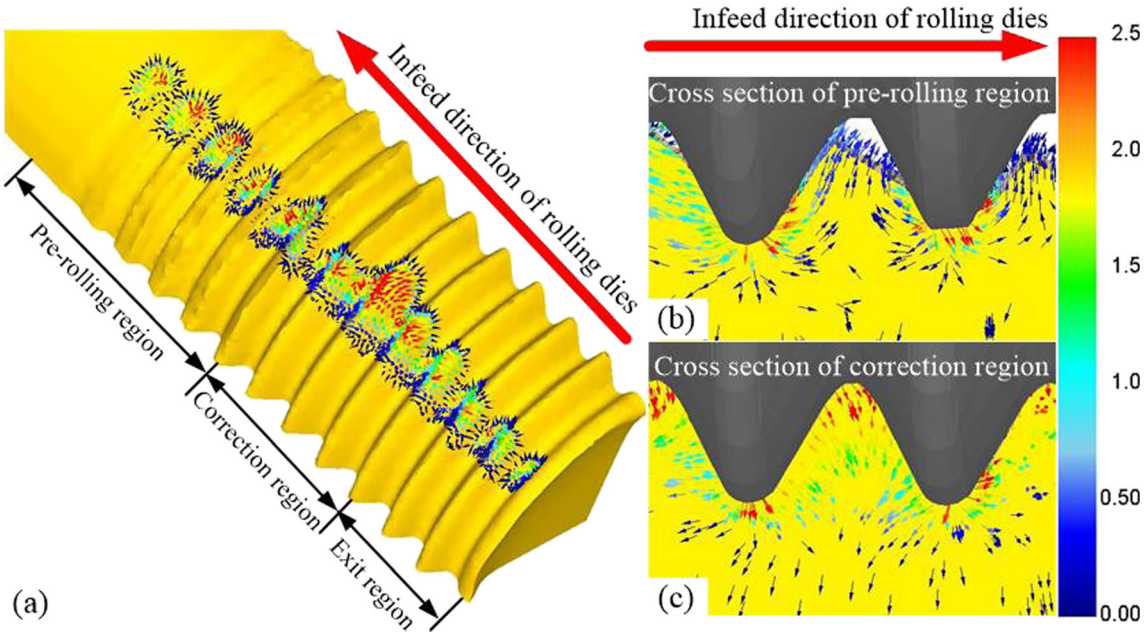

Fig. 12 The distribution of material flow. (a) material flow on surface, (b) material flow in pre-rolling region, and (c) material flow in corretion region

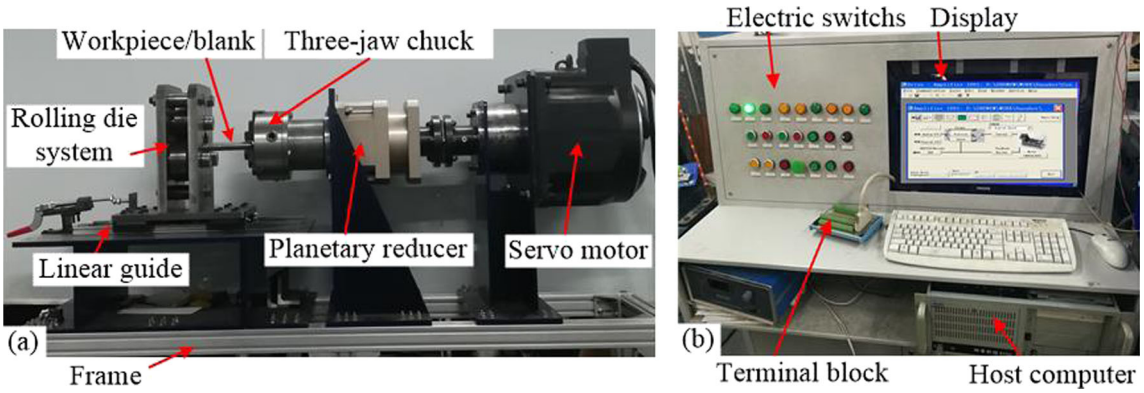

Fig. 13 The formed equipment of thread shaft: **a** the mechanical part of formed equipment and **b** the control part of formed equipment.

and which accumulates on the tooth profile; therefore, the axial and radial displacement is larger than that in tooth space. And along the radial inward direction, the equivalent strain and displacement are decreased.

Figure 12 shows the material flow distribution in the self-infeed rolling process. Figure 12 (a) shows the velocity distribution of thread shaft surface. In the pre-rolling region, the addendum of rolling dies contacts with workpiece and forms the tooth space; therefore, the material flow mainly occurs in the bottom of the tooth space. In the correction region, the material flow occurs both in the bottom of tooth space and the top of tooth profile. The material flow in the top of tooth profile is larger than that in the bottom of tooth space. In the exit region, the material flow is weak for the reason of that the tooth shape has been formed.

Figure 12 (b) and (c) show the material flow in the cross section of pre-rolling region and correction region. In the pre-rolling region, the material flows along the flank of rolling die from the bottom of tooth space to the top of tooth profile. While for the rolling die along the two sides of the tooth space, the material flow velocity is different leading to the difference of the deformation degree of tooth profile. In the correction region, the addendum of thread shaft contacts with the dedendum of rolling die, and the top of tooth profile is calibrated. The material flow occurs in the top of tooth profile and the bottom of the tooth space, with the former relatively larger than the latter. In the surface layer of thread shaft, the direction of material flow is opposite to that on the surface of rolling die. In the core region of thread shaft, the material flows along inward direction but the speed is very small.

The material flow well agrees with the displacement distribution and the equivalent strain distribution. In the pre-rolling region, the material flow starts from the bottom of tooth space to the top of tooth profile. In the correction region, the material flows toward the internal of tooth profile.

Table 2 Material properties of AISI 1045

Property	σ_s/MPa	σ_b/MPa	δ/%	ψ/%	μ	E/GPa
Value	417.6	620.2	18.6	39.8	0.3	210

4 The experimental verification of self-infeed rolling process for thread shaft

4.1 The experiment processes and parameters

The experiments of self-infeed rolling process for thread shaft were implemented with special processing equipment which includes four parts: the driving part, the control system, the fixing part, and the rolling die system. The driving part is composed of a servo motor and a planetary reducer which drive the blank rotated with the desirable speed and which is controlled by the control system. The fixed part mainly contains a three-jaw chuck for clamping the bank. The rolling die system consists of three rolling dies and the locating devices. Parts of equipment are shown in Fig. 13. In these experiments, the blank material is medium carbon steel AISI 1045 and the material properties are listed in Table 2. The speed of servo motor is 50 r/min, and the speed of blank is 10 r/min. When the blank is rotating, the rolling die system moves along the linear guide. The axial self-infeed velocity is determined by the rotating speed of the blank.

4.2 The experiment result

After the experimental processes, the thread shafts were cut apart along the axis by wire-electrode cutting and made them into samples. The change of thread shaft forming process was observed and the pitch and tooth angle were measured by microscope (Leica DMI3000M metallographic microscope).

Figure 14 shows the comparison results of finite element analysis and the experiments. The results of finite element analysis are well coincided with the experiments. In the forming process of thread shaft, the height of tooth profile is gradually increasing. There are two protrusions on both flanks of tooth profile, but the protrusion in region I is taller than that

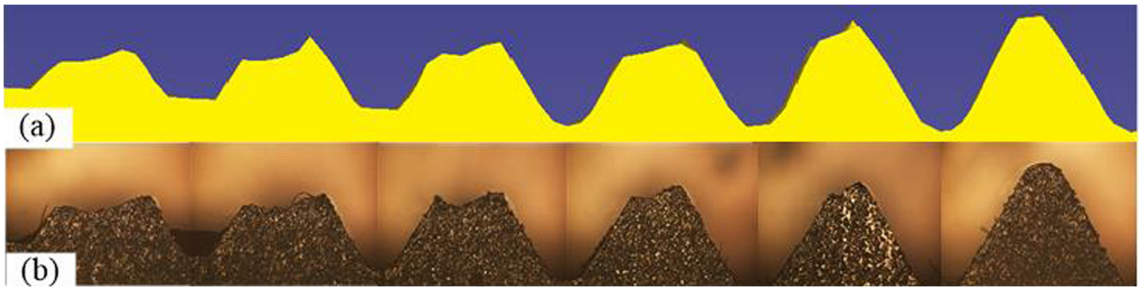

Fig. 14 The comparison of finite element analysis and experiments: (a) the finite element analytical results and (b) the experimental results

in region II which indicates region I has larger deformation (the right flank is in region I and the left flank is in region II, in Fig. 14). This phenomenon can be used to check the uneven strain state on tooth profile.

The thread pitch and tooth angle were also measured by microscope and the results are shown in Fig. 15. The distance between two thread teeth is 2999.68 μm and the tooth angle is 59.22°, which are well agreed with the demands of thread pitch 3 mm and tooth angle 60°. It illustrates the accuracy of formed tooth profile and the feasibility of self-infeed rolling process of thread shaft.

4.3 The improvement of microstructure of the formed thread shaft

The sample is polished, and corroded by 4% nitric acid alcohol solution, and then it is observed by optical microscope. The microstructure of the formed thread shaft with AISI 1045 is shown in Fig. 16. The microstructure mainly contains pearlite and ferrite in the center of thread component. The color of pearlite is dark which distributes as net shape. The color of ferrite is brighter which distributes as flaky.

The grains in the bottom of tooth root region and the surface layer of tooth profile are stretched which forms the fibrous tissue. The fibrous tissue's grain is obviously refined and dense, and the flow line is distributed along the direction of the tooth surface which can improve the distributed uniformity of structure and increase the shear and fatigue strength of the formed thread shaft [6].

Through the forming process, the grains in the top, flank, and bottom of the tooth profile are fractured, dense, and refined. The average sizes are counted and which in the top, flank, and bottom of tooth profile respectively are 12.066 μm, 11.992 μm, and 11.56 μm. In the center of thread shaft, the average grain size is 12.866 μm. The maximum reduction of grain size is 10.15%. The refined grains can enhance the strength of thread shaft based on the Hall–Petch theory. With the increase of inward depth from the tooth surface to the center, the refined and fibrous tissue disappeared and the grain size increased.

4.4 The hardness distribution of the formed thread shaft

Forming process can influence the hardness of thread shaft, and the results of the strain state and microstructure of the deformed thread shaft can be checked by hardness characteristics; therefore, it is meaningful to investigate the hardness distribution. A micro-sclerometer (Type: HVT-100A, HV standard) was used to measure the hardness of the formed thread shaft. The measured position is displayed in Fig. 17. The points P11, P12, P13, P14, P15, and P16 are along outward radially. The points P21, P22, P23, and P24 are located on the flank of tooth profile in region I. The points P31, P32, P33, and P34 are located on the other flank of tooth profile in region II. The hardness of each point was measured three times and the average value was selected as the evaluation.

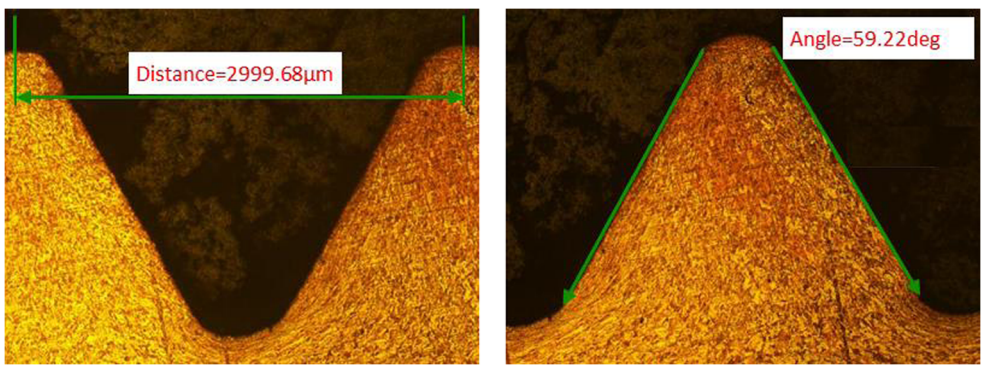

Fig. 15 The measured result of thread tooth profile

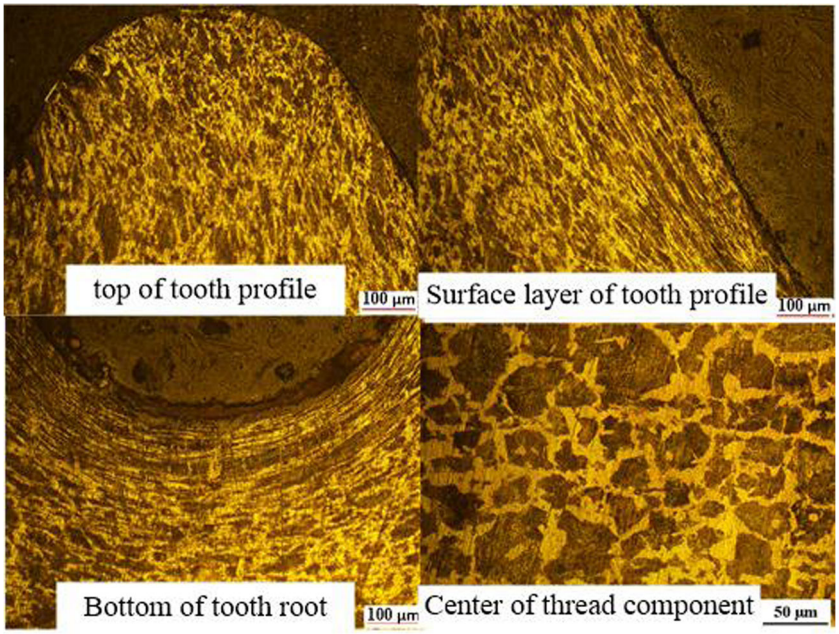

Fig. 16 The microstructure of formed thread shaft

The values of hardness are shown in Fig. 18. Along the radial outward direction (from P11 to P16), the strain increases and the grain is refined, so the hardness gradually increase from 229.8 to 264.5. On the tooth profile, the strain on both flanks is larger than that in the middle of the tooth profile and which in region I is larger than that in region II. The microstructure is fibrous tissue and the grain is refined on both flanks. So, the average value of hardness on the flank in region I (from P21 to P24) is 288.4 and which in region II (from P31 to P34) is 281.2. The hardness on flanks is larger than that in the middle of tooth profile and which on the flank in region I is slight larger than that in the region II. At the bottom of the tooth space, the maximum strain appears and the microstructure is obviously streamlined and dense. So the hardness is 298.1 which is the largest. Comparing with the hardness of blank, the hardness at the bottom of the tooth space is improved to 29.7%. The hardness distribution is consistent with the equivalent strain distribution and microstructure characteristics.

5 Conclusion

Based on the above analysis on the self-infeed rolling process, the conclusions are listed as follows:

1) For the axial motion of rolling dies, the rolling dies squeeze one flank of tooth profile which leads to the deformation degree of region I is larger than that of region II. The maximum equivalent strain is located on the

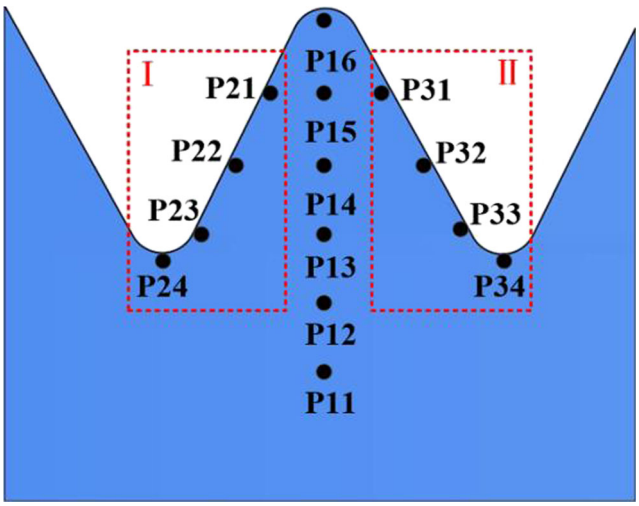

Fig. 17 The measured position of hardness

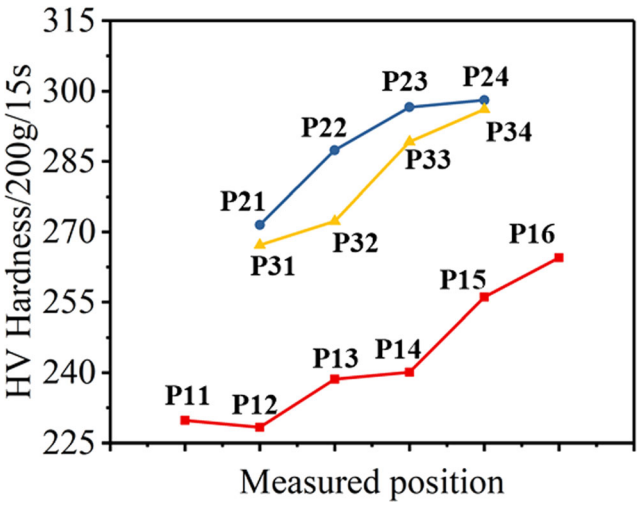

Fig. 18 The hardness distribution of the formed thread shaft

bottom of tooth space which decreases along the inward radial direction.

2) On the surface layer, the radial displacement of material is larger than axial displacement. During the rolling process, the material flow starts from the bottom of tooth space to the top of tooth profile which leads to the tooth being gradually taller.
3) Through the self-infeed rolling process, the grains are refined and the maximum reduction of grain size is up to 10.15%. The microstructure in the surface layer and the bottom of tooth space is fibrous tissue which is dense and streamlined.
4) The hardness of surface layer and root of tooth is obviously increased. The maximum improvement of hardness is 29.7%. And the hardness distribution is well according to the equivalent strain distribution and microstructure characteristics.

Funding This work was supported by the State Key Laboratory of Materials Processing and Die & Mould Technology, Huazhong University of Science and Technology (Grant No. P2019-028) and National Natural Science Foundation of China for key Program (Grant No. 51335009).

References

1. Cui MC, Zhao SD, Zhang DW, Chen C, Fan SQ, Li YY (2017) Deformation mechanism and performance improvement of spline shaft with 42CrMo steel by axial-infeed incremental rolling process. Int J Adv Manuf Technol 88(9-12):2621–2630
2. Cui MC, Zhao SD, Zhang DW, Chen C, Li YY (2016) Finite element analysis on axial-pushed incremental warm rolling process of spline shaft with 42CrMo steel and relevant improvement. Int J Adv Manuf Technol 90(9-12):2477–2490
3. Kamouneh AA, Ni J, Stephenson D, Vriesen R (2007) Investigation of work hardening of flat-rolled helical-involute gears through grain-flow analysis, FE-modeling, and strain signature. Int J Mach Tool Manu 47(7-8):1285–1291
4. Zhuang X, Sun X, Xiang H, Xia M, Zhao Z (2016) Compound deep drawing and extrusion process for the manufacture of geared drum. Int J Adv Manuf Technol 84(9-12):2331–2345
5. Tschätsch H (2006) Metal forming practise, translated by Koth a. Springer, Berlin Heidelberg
6. Song JL, Liu ZQ, Li YT (2012) Theory and technology of precise cold rolling forming of shaft part. Defense Industrial Press, Beijing (in Chinese)
7. Martin JA (1998) Fundamental finite element evaluation of a three dimensional rolled thread form: modelling and experimental results, fatigue, fracture, and residual stresses. ASME 373:457–467
8. Domblesky JP, Feng F (2002) A parametric study of process parameters in external thread rolling. J Mater Process Technol 121(2–3):341–349
9. Domblesky JP, Feng F (2002) Two-dimensional and three-dimensional finite element models of external thread rolling. Proc Inst Mech Eng B J Eng Manuf 216(4):507–517
10. Pater Z, Gontarz A, Weronski W (2004) New method of thread rolling. J Mater Process Technol 153–154:722–728
11. Chen CH, Wang ST, Lee RS (2005) 3-D finite element simulation for flat-die thread rolling of stainless steel. J Chin Soc Mech Eng 26(5):617–622
12. Lee MC, Jang SJ, Han SS, Yoon DJ, Joun MS (2010) New finite-element model of thread rolling. Steel Res Int 9:214–217
13. Qi HP, Li YT, Fu JH, Liu ZQ (2008) Minimum wall thickness of hollow threaded parts in three-die cold thread rolling. Int J Mod Phys B 22:6112–6117
14. Qi HP, Li YT, Liu ZQ (2011) Numerical simulation study on the cold rolling of hollow thread. Adv Mater Res 160(162):849–854
15. Yamanaka S, Amiya K, Saotome Y (2014) Effects of residual stress on elastic plastic behavior of metallic glass bolts formed by cold thread rolling. J Mater Process Technol 214(11):2593–2599
16. Nitu E, Tabacu S, Iordache M, Lacomi D (2013) Finite element analysis and experimental validation of the wedge rolling process. Proc Inst Mech Eng B J Eng Manuf 227(9):1325–1339
17. Zhang DW, Zhao SD, Ou H (2016) Analysis of motion between rolling die and workpiece in thread rolling process with round dies. Mech Mach Theor 105:471–494
18. Zhang DW, Zhao SD (2014) New method for forming shaft having thread and spline by rolling with round dies. Int J Adv Manuf Technol 70(5-8):1455–1462
19. Zhang DW, Zhao SD (2016) Deformation characteristic of thread and spline synchronous rolling process. Int J Adv Manuf Technol 87(1-4):835–851
20. Zhang DW, Zhao SD, Wu SB, Zhang Q, Fan SQ, Li JX (2015) Phase characteristic between dies before rolling for thread and spline synchronous rolling process. Int J Adv Manuf Technol 81(1):1–16
21. Zhang DW, Cui MC, Cao M, Ben NY, Zhao SD (2017) Determination of friction conditions in cold-rolling process of shaft part by using incremental ring compression test. Int J Adv Manuf Technol 91(9-12):3823–3831